Iranian Journal of Science & Technology, Transaction A, Vol. 30, No. A1
Printed in The Islamic Republic of Iran, 2006

FLUORINE AND CHLORINE IN BIOTITE FROM THE SARNWOSAR GRANITIC ROCKS, NORTHEASTERN IRAN*

M. BOOMERI[1**], T. MIZUTA[2], D. ISHIYAMA[2], AND K. NAKASHIMA[3]

[1]Dept. of Geology, University of Sistan and Baluchestan, Zahedan, I. R. of Iran
Email: boomeri@hamoon.usb.ac.ir
[2]Institute of Applied Science, Akita University, Akita, Japan
[3] Dept. of Earth Sciences, Faculty of Science, Ymagata University, Yamagata, Japan

Abstract – The late Eocene-early Oligocene Sarnowsar granitic rocks and many dacitic to rhyolitic dykes intruded in metamorphosed and metasomatized shale, sandstone, calcite and dolomite marbles and volcaniclastic and pyroclastic rocks. As a result several million tons of iron ores formed within carbonate rocks in the Sangan area. The Sarnowsar granitic rocks are mainly granite to granodiorite, metaluminous, I type and high calc-alkaline.

Fluorine contents in the biotite range from 0.37 to 4.4 wt. % and Cl contents range from 0.1 to 0.30 wt. %. Fluorine contents in the biotite are negatively correlated with X_{Ti}, while Cl contents positively correlated with X_{Mg} and X_{Si}.

Values of the calculated log (fH_2O/fHF) and log ($fH_2O/fHCl$) of fluid in equilibrium with the chemical composition of biotite range from 3.38 to 4.43 and 0.57 to 1.2, respectively. The contour lines representing log (fH_2O/fHF) and log ($fH_2O/fHCl$) values are different with the slope of the trend of biotite composition suggesting that, in addition to chemical structure of biotite, the fluid composition also plays some role in the incorporation of F, and especially Cl in biotite. The F intercept values for biotite in the Sarnowsar granitic rocks are similar to those of igneous rocks and porphyry Cu ore deposits. The Cl intercept values of biotite in the Sarnowsar granitic rocks are similar to those of hydrothermal and ore forming systems. The data suggest that chlorine intercept values for biotite from the Sangan deposit tend to be more Cl rich than comparable values from biotites in common igneous rocks. F-rich biotites and F-poor biotites from the Sangan deposit show similar and narrow ranges of F/Cl intercept values corresponding to Cl-rich and ore-forming systems such as porphyry copper deposits. Therefore, the chemical composition of biotite from the Sarnowsar granitic rocks interacted with hydrothermal solutions.

Keywords – Iran, Sarnowsar granitie, Biotite, F and Cl, *f*HF, *f*HCl, IV(F), IV(Cl)

1. INTRODUCTION

The chemical composition of biotite in a mineralized granitoid may represent the confluence of many chemical and physical factors including the concentration of water, halogens, and ore metal and magma oxidation states, volatile phase exsolution, etc. Because distribution of F and Cl between granitic magmas and magmatic hydrothermal fluids strongly affects metal ratio, the order of crystallization, the timing of vapor saturation and mass transport in the magmatic hydrothermal fluids and hydrothermal ore deposition. F and Cl bearing fluids are also responsible for the alteration of granitic rocks and their host rocks [1-4].

Biotite is contained between 70 to 90 % F in muscovite-and fluorite-free granitoid rocks, the remainder is in apatite and sphene [5]. The behavior of F in biotite is key to the behavior of F in many

*Received by the editor September 25, 2004 and in final revised form December 7, 2005
**Corresponding author

igneous rocks. It was experimentally indicated that the substitution of F or Cl in the hydroxyl site of mica is controlled by the activity of F or Cl, composition of mica and temperature [6, 7, 1]. They suggested that Mg-rich micas incorporate more F than Fe-rich micas under similar conditions. Such relations have been termed Fe-F avoidance principle [8, 9]. This principle has been confirmed in natural micas [10-13, 5, 1, 2, 14-21].

F and Cl in biotite in the Sarnowsar granitic rocks will be considered in this paper. This is a good case study because a huge iron skarn deposit was formed due to the hydrothermal activity of the Sarnowsar granitic rocks. The Sarnowsar granitic rocks close to the Sangan iron deposit are located 300 km southeast of Mashhad, northeastern Iran.

2. GEOLOGICAL SETTING

Iran is geologically composed of many structural zones that show different characters (Fig. 1). The Zagros thrust zone, mainly composed of sedimentary rocks with continuous deposition until the Pliocene. The Sanandaj-Sirjan zone is mainly a metamorphic zone composed of Mesozoic intrusions and metamorphosed sediments. The Sahand Bazman magmatic belt is mainly composed of plutonic and volcanic rocks of the Oligo-Miocene age. Central Iran is a complex zone of many rock types from Precambrian to present. The old core of Iran contains bimodal igneous rocks of Precambrian cover by Paleozoic rocks. The Alborz Mountains closed a paleotethys located to the north of Iran. The Kope Dagh is a non-volcanic sedimentary basin composed of a complete Mesozoic-Tertiary stratigraphic sequence. The Makran zone is an accretionary prism composed of flysch-mollasse type sediments of post-Cretaceous. All these zones were formed by opening and closing of Paleo and Neotethys oceanic basins due to subduction and collision events in the south and north of Iran. The north side of Iran collided with Turkmenistan or the Turan plate (Urasia) in late Triassic-early Jurassic time [23]. By the south, Iran was subducted and collided with the Arbia plate starting from late Cretaceous [23] and continuing to Miocene and later times [24, 25]. The Sarnowsar granite is introduced as a part of Central Iran (Fig. 1), but similar rocks are scattered in many parts of Iran such as Alborz, Central Iran and Sahand-Bazman zones. Eocene calc-alkaline volcanic and pyroclastic rocks and the Eocene-Oligocene calc-alkaline felsic intrusives of the continental arc in the Sangan area appear to be a part of an extensive volcanism and magmatism [26] that started in the Eocene period (50 Ma) and continued to a climax during the middle Eocene (about 47-42 Ma) for volcanic rocks and late Eocene for plutonic rocks in many parts of Iran. [23]. These types of volcanic and plutonic rocks are generally associated with extensive porphyry copper and skarn mineralization such as Sungon [27], Sarchesmeh, Mieduk and many other sub economical ore bodies in the Sahand-Basman zone and the Sangan Iron skarn deposit in northeastern Iran [26] .

The Sarnowsar granite is located in a quadrangle map of Taybad [28] and Khaf [29]. The area is composed of numerous formations from Precambrian until present day. The sedimentary rocks were attributed to late Proterozoic in the area [28] (Fig. 2-a). Recent studies show the granitic batholith (Sarnowsar granite) and many dacitic to rhyolitic dykes intruded in lower Jurassic contact metamorphosed and metasomatized shale, siltstone and sandstone, Middle to Upper Cretaceous calcite and dolomite marbles and Eocene volcaniclastic and pyroclastic rocks (Fig. 2) [26]. The granitic rocks belong to the late Eocene-early Oligocene ages [28].

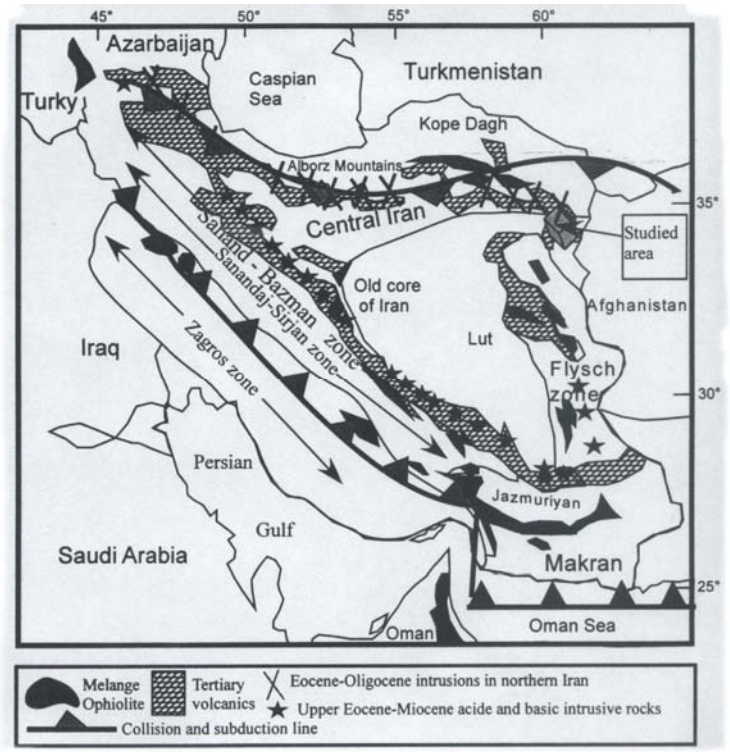

Fig. 1. Generalized geological map showing major structural zones of Iran and distribution of volcanic and plutonic rocks [3, 22]

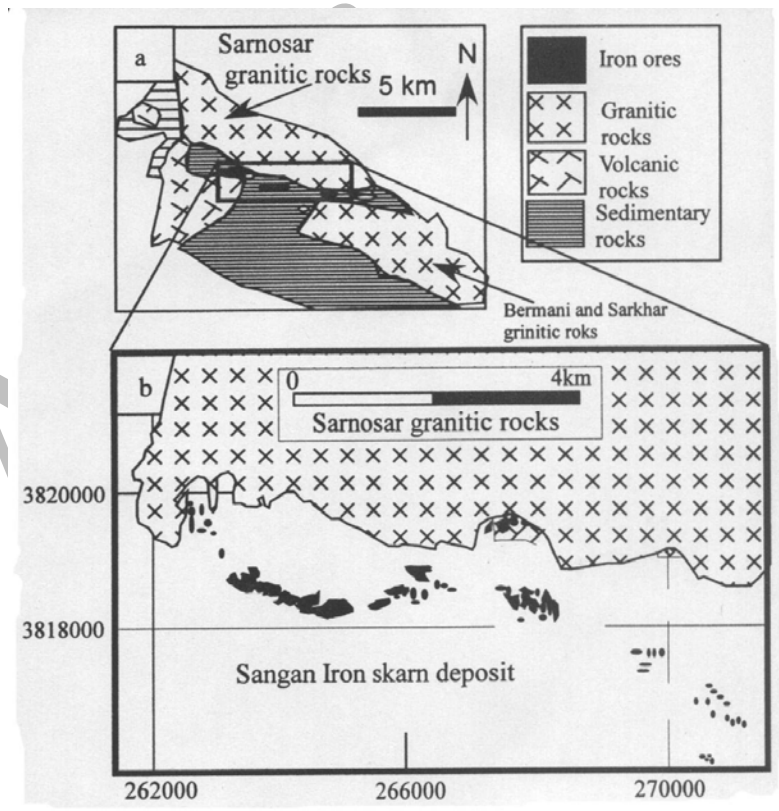

Fig. 2. Simple geological maps showing the distribution of the Sarnowsar granitic and iron ores in the Sangan deposit

3. PETROGRAPHY AND GEOCHEMISTRY

The Sarnowsar granitoid is a part of many intrusive rocks in the area with a strike W-E (Fig. 2), mainly occurring as a medium gray and medium grained linear batholiths associated with some granitic, pegmatitic and aplitic stocks and dykes. Their apophyses intruded on some parts of the Sangan iron deposit and ranges from alkali granite to granodiorite with granular, porphyritiic, aplitic and pegmatitc textures. The Sarnowsar granitic rocks are mainly composed of quartz, K-feldspar, Plagioclase, biotite and ± amphibole and accessory minerals of sphene, magnetite, apatite, and zircon with or without ilmenite, pyrite, chalcopyrite and hematite. The granitic rocks consist of abundant xenoliths with microgranular and porphyritic textures. The xenoliths are intermediate in composition. The feldspars are partially altered to sericite and kaolinite. The amphiboles are edenite and actinolite and are partially replaced by sphene, magnetite and biotite[26]. Primary sphene associated with magnetite in the Sarnowsar granite is an indicator of a high oxidizing condition [30].

Biotite is the most abundant ferromagnesian mineral in the Sarnowsar granite. It varies in size, shape and texture. Some biotites are zoned and some of them are replaced by magnetite and quartz. The biotite is slightly altered to chlorite in rims [26].

Chemical compositions of samples of the Sarnowsar granite were determined by Rigaku 3270 XRF (X-ray fluorescence) at Akita university of Japan for major elements and by potentiometric titration for FeO and H_2O. Modal composition of minerals in the Sarnowsar granite was obtained by point counting of minerals in thin slabs. The representative result is given in Table 1.

Table 1. Representative major element chemical analyses of the Sarnwsar granitic rocks

Samples (wt %)	G1A	DG1	SG3	SG1	SG2	G1B	G82
SiO_2	67.9	69.1	70.0	74.8	74.8	67.0	68.8
TiO_2	0.6	0.5	0.5	0.3	0.2	0.7	0.5
Al_2O_3	15.3	14.3	14.7	12.7	12.8	15.5	15.0
Fe_2O_3	1.9	2.0	1.9	0.4	0.8	1.8	1.0
FeO	1.8	1.1	0.8	1.1	1.2	2.2	2.0
MnO	0.0	0.0	0.0	0.0	0.0	0.0	0.0
MgO	1.1	0.8	0.5	0.4	0.4	1.2	1.1
CaO	2.3	2.3	1.2	0.8	1.1	2.5	2.2
Na_2O	3.9	3.6	4.1	2.6	3.0	4.0	4.3
K_2O	4.2	4.6	5.2	5.7	5.0	3.9	4.6
P_2O_5	0.2	0.1	0.1	0.1	0.1	0.2	0.2
H_2O^+	0.2	0.6	0.3	0.8	0.5	0.6	0.0
H_2O^-	0.1	0.2	0.3	0.4	0.1	0.3	0.1
Total	99.5	99.2	99.7	99.9	99.9	99.9	99.9
ASI	1.0	1.0	1.0	1.1	1.0	1.0	0.9
F in biotite	0.9	2.0	1.9	4.1	2.7	0.8	2.1
Modal % Biotite	6.2	3.7	4.2	0.3	3.3	6.6	2.0
Modal % plg	43.2	19.8	25.2	28.2	29.3	39.4	25.3

The pluton is metaluminous, I type ($Al_2O_3/(CaO + Na_2O + K_2O) < 1.1$) and has a high content of alkali ($Na_2O + K_2O$) > 8 wt %), high concentration of light REE, F-rich biotite and fluorapatite. Some geochemical features of the Sarnowsar granitic rocks are shown in Table 2. Using Al as an amphibole barometer, the lithostatic pressure is less than 2.5 kb [26].

Table 2. Chemical features of Sarnowsar granite

SiO_2 (wt %)	63-75
Magmatic series	High-calc-alkaline
$Al_2O_3/(Na_2O + K_2O)$	1.15-1.35
Na_2O/CaO	1.4-3.4
Na_2O/K_2O	<1
MgO/FeO	0.18-0.38
MgO/MnO	13-39
Shand`s index	Metaluminous

Quartz in samples from the granite contains fluid inclusions with one, two and several daughter minerals associated with vapor rich inclusions. The fluid inclusion homogenized in a wide range of temperatures from 140 to above 510° C. The salinities obtained for these fluid inclusions range from 30 to 70 % NaCl equivalent [26].

The felsic dykes are dacitic to rhyolitic with porphyritic textures. Their K_2O content is very high (> 6 %) partly due to K metasomatism [26]. The granitic rocks and Eocene volcanic rocks in the area show similar trends on petrogenetic variation and discrimination diagrams. They appear to belong to a high calc-alkaline magmatic series which probably evolved in an arc-continental tectonic setting. The geology and mineralogy of granite and the chemical composition of biotite indicate that the pluton is an oxidized epizonal type [26]. The granitic rocks in the system Q-Ab-An-H_2O tend to lower temperature minimum points, indicating high water pressure. The characteristics of the Sarnowsar granitic rocks show that the melt contained enough water and volatiles to generate a magmatic aqueous phase during crystallization and emplacement of the melt in the shallow crust [26].

4. ANALYTICAL METHOD

The microanalyses of biotite in the Sarnowsar granite were conducted by an automated JEOL. JXA-8600 Superprobe of Yamagata University with an accelerating voltage of 15 KV and a beam current of 2×10^{-8} A. The following standards were used for X-ray microanalyses: apatite, wollastonite, albite, adularia, synthetic SiO_2, TiO_2, Al_2O_3, Cr_2O_3, Fe_2O_3, MnO, MgO, CaF_2 and NaCl. The diameter of a focused electron beam is about 5 μm. Data were processed by an on-line computer using the Oxide ZAF in the XM-86 PAC program composed by JEOL. The Biotite formula is based on the 22 oxygens and OH is calculated on OH= 4-(Cl + F). Total iron in biotite is assumed as Fe^{2+}.

5. RESULTS

The chemical compositions of some analyzed biotites in the Sarnowsar granite are given in Table 3. Other data are from [26] and are only shown in the Figs. Biotite in the Sarnowsar granite shows variation in composition. It is mainly Mg rich and some of them are phlogopite in composition (Fig. 3), however all of them are optically typical biotite. F contents in the biotite range from 0.37 to 4.4 wt. %, whereas Cl contents range from 0.1 to 0.31 wt. %, F is strongly correlated with cations in octahedral and also in tetrahedral sites of the biotite. The contents of F in biotite are negatively correlated with X_{Ti} and Cl contents (Fig 4). It is positively correlated with X_{Mg} and X_{Si} (Fig. 4). Regarding negative correlation of F and Cl contents in biotites, the relationships are inverse with Cl contents of biotite (Fig. 4).

Table 3. Representative EPMA analyses of biotite from the Sarnowsar granite

Samples	NG5	A'G7	G1B8	G1A	SG1	DG2	ND2	DG1	G7-5	SG2	G81
SiO_2	37.87	37.87	37.70	38.32	41.92	39.10	40.70	39.32	42.10	39.66	42.18
TiO_2	3.75	5.42	4.01	4.46	1.51	4.14	2.20	3.69	2.31	3.69	1.41
Al_2O_3	12.67	13.74	13.20	13.30	12.20	12.98	11.72	13.02	11.58	13.16	11.04
FeO	19.36	16.12	19.79	18.79	12.89	16.26	14.10	14.83	10.76	15.40	10.68
MnO	0.32	0.28	0.31	0.29	0.56	0.11	0.17	0.35	0.33	0.36	0.50
MgO	12.40	14.07	12.63	12.61	16.37	14.92	17.39	15.67	19.50	15.56	18.57
Na_2O	0.14	0.59	0.18	0.15	0.04	0.05	0.05	0.26	0.18	0.13	0.40
K_2O	9.54	9.09	9.77	9.62	9.53	9.64	9.63	9.73	9.61	9.80	9.76
F	0.82	2.45	0.63	0.91	4.14	1.13	2.15	1.95	3.26	2.72	4.39
Cl	0.23	0.17	0.24	0.25	0.10	0.16	0.16	0.20	0.13	0.16	0.12
H_2O	3.46	2.75	3.61	3.49	2.27	3.45	2.92	3.02	2.44	2.66	2.16
O	-0.42	-1.13	-0.33	-0.46	-1.76	-0.54	-0.99	-0.91	-1.48	-1.24	-1.88
Total	100.14	101.44	101.73	101.73	99.79	101.38	100.20	101.14	100.71	102.05	99.34
Numbers of cations on the basis of 22 O											
Si	5.808	5.737	5.696	5.764	5.910	5.829	6.136	5.905	6.278	5.957	5.92
Al^{IV}	2.192	2.263	2.304	2.236	2.030	2.171	1.864	2.095	1.722	2.043	1.83
Ti	0.000	0.000	0.000	0.000	0.070	0.000	0.000	0.000	0.000	0.000	0.15
Tot tet.	8.000	8.000	8.000	8.000	8.000	8.000	8.000	8.000	8.000	8.000	8.00
Al^{VI}	0.099	0.190	0.048	0.123	0.000	0.111	0.218	0.210	0.315	0.288	0.00
Ti	0.432	0.617	0.455	0.504	0.090	0.464	0.249	0.417	0.259	0.416	0.00
Fe	2.482	2.042	2.501	2.364	1.520	2.027	1.778	1.863	1.343	1.935	1.25
Mn	0.041	0.036	0.039	0.037	0.070	0.013	0.022	0.044	0.041	0.046	0.06
Mg	2.835	3.177	2.844	2.828	3.440	3.314	3.907	3.508	4.333	3.484	3.89
Tot 0ct.	5.889	6.062	5.887	5.856	5.120	5.929	6.174	6.043	6.290	6.169	5.20
Na	0.043	0.174	0.051	0.043	0.010	0.015	0.015	0.076	0.052	0.037	0.11
K	1.866	1.758	1.884	1.846	1.710	1.833	1.852	1.865	1.829	1.878	1.75
A site	1.909	1.931	1.935	1.890	1.720	1.848	1.867	1.941	1.881	1.915	1.86
F	0.398	1.173	0.301	0.432	1.840	0.534	1.027	0.924	1.538	1.291	1.95
Cl	0.060	0.044	0.062	0.064	0.020	0.039	0.041	0.052	0.034	0.040	0.03
OH	3.542	2.782	3.637	3.504	2.130	3.426	2.932	3.024	2.428	2.669	2.02
$Log(X_F/X_{OH})$	-0.950	-0.375	-1.083	-0.910	-0.060	-0.807	-0.456	-0.515	-0.198	-0.315	-0.02
$Log(X_{Cl}/X_{OH})$	-1.773	-1.799	-1.767	-1.736	-1.970	-1.939	-1.849	-1.764	-1.858	-1.822	-1.83
$Log(fH_2O/fHF)$	3.969	3.432	4.096	3.925	3.380	3.918	3.670	3.651	3.480	3.433	3.37
$Log(fH_2O/fHCl)$	0.985	0.929	0.976	0.945	1.020	1.001	0.769	0.785	0.669	0.873	0.53
IV(F)	1.869	1.332	1.996	1.825	1.220	1.818	1.570	1.551	1.380	1.333	1.27
IV(Cl)	-4.166	-4.222	-4.175	-4.206	-4.280	-4.150	-4.382	-4.366	-4.482	-4.278	-4.63
IV(F/Cl)	6.031	5.551	6.168	6.027	5.500	5.964	5.947	5.914	5.858	5.607	5.89
X_{sid}	0.138	0.180	0.171	0.165	0.073	0.112	0.011	0.105	0.000	0.110	0.00
X_{an}	0.381	0.296	0.346	0.353	0.320	0.329	0.356	0.314	0.326	0.325	0.29
Mg/(Mg+Fe)	0.533	0.609	0.532	0.545	0.694	0.620	0.687	0.653	0.763	0.643	0.76

Total Fe as FeO, H2O was calculated by assuming OH=4-(F+Cl), IV is intercept value

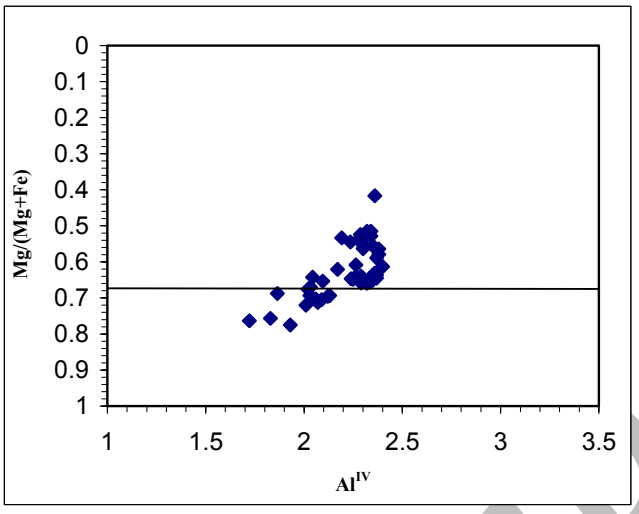

Fig. 3. Mg/(Mg+Fe) versus Al^{IV} of biotite from the Sarnowsar granite

Positive relationship of Mg contents with F contents in biotite from the Sangan deposit can also be due to the Fe-F avoidance principle. This is because the relationship with moles of Mg in the octahedral site is very strong (Fig. 4).

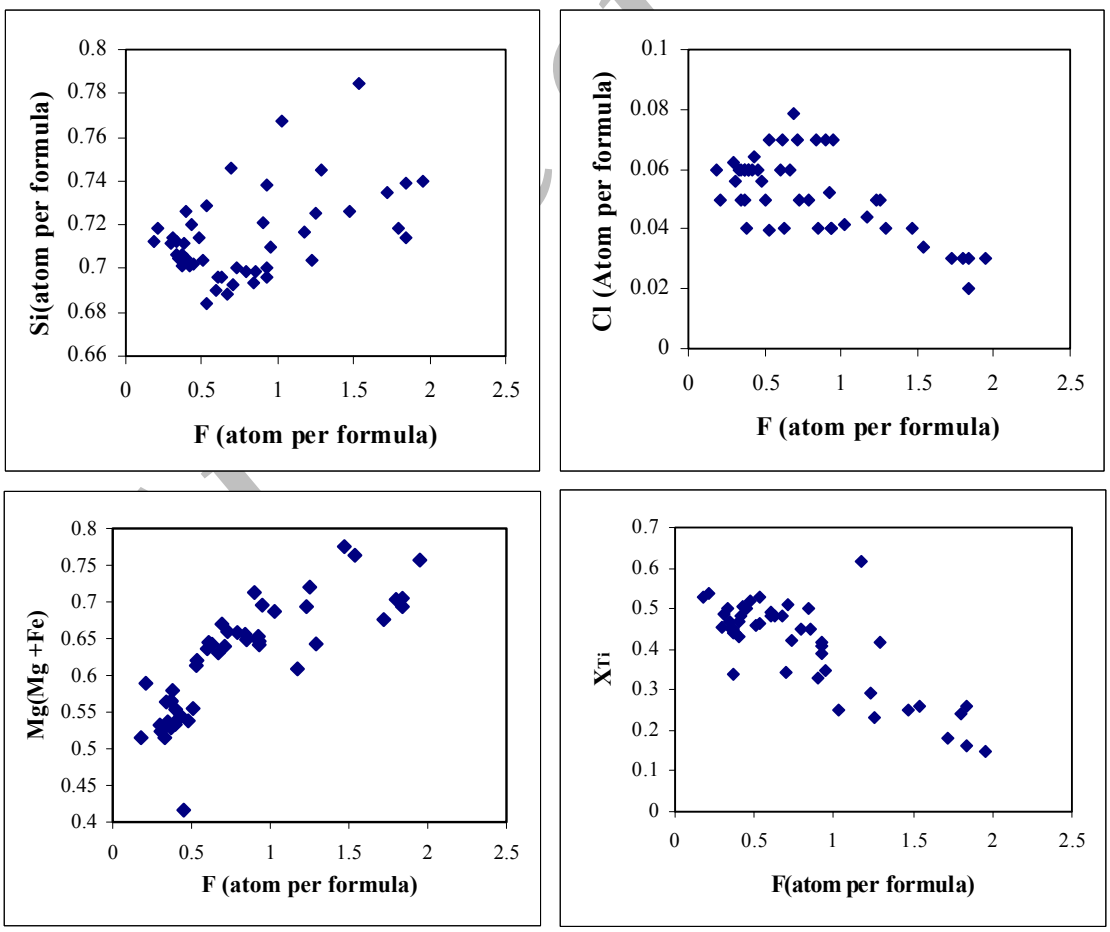

Fig. 4. Relationships of F and Cl (Atom per formula) with Mg/Mg+Fe and X_{Ti} in octahedral site and X_{Si} in tetrahedral site of biotite from the Sarnowsar granite

6. HALOGEN FUGACITY

Exchange equilibrium between a mica and either a silicate melt or aqueous fluid phase permits the calculation of halogen fugacity by following exchange reactions: mica (OH) + HX = mica (X) + H_2O [1], where X stands for either F or Cl. The log of the equilibrium constant K for their exchange reaction is:

$$\log K = \log (a_X/a_{OH}) + \log(a_{H_2O}/a_{HX})$$

where a_X and a_{OH} are the activities of halogen and hydroxyl components present in the solid solution of micas, and a_{H_2O} and a_{HX} are the activities of H_2O and HF or HCl present in the magma or fluid. A standard state of pure H_2O and HX are assumed. The activities could then be converted to fugacity at 1 bar and the temperature of interest [1]. Munoz and Ludington [31, 6] experimentally measured the equilibrium constants of F = OH exchange for synthetic phlogopite, annite, and siderophyllite. From these experiments, it is possible to calculate both temperature and the effect of composition on the equilibrium constant [1].

The simultaneous mixing of (Mg, Fe^{2+}) and (F, OH) in a homogeneous biotite solution, expressed in terms of the following exchange reaction can be considered

$$K_2Mg_6(Si_6Al_2O_{20})(OH)_4+K_2Fe_6(Si_6Al_2O_{20})F_4=K_2Mg_6(Si_6Al_2O_{20})F_4+K_2Fe_6(Si_6Al_2O_{20})\ OH)_4$$

(OH-phlogopite) + (F-annite) = (F-phlogopite) + (OH-annite)

Where

$$\log K = \log Kph - \log KAn = 1.107 \text{ [1].}$$

The following equation was derived using experimental and thermodynamic data [1].

$$\log K = 2100/T + 1.523\ X_{Mg} + 0.416X_{An} + 0.\ 2X_{Sid} = \log(fH_2O/fHX) + \log(X_F/X_{OH}).$$

The mole fraction of siderophyllite (X_{Sid}) and mole fraction of annite (X_{An}) in biotite were obtained from equations of Gunow et al. [32].

By assuming a formation temperature of 727°C (the estimated temperature for biotite in the granite [33] this study used Munoz's equations to calculate log (fH_2O/fHF) and log ($fH_2O/fHCl$) for fluids in equilibrium with F-bearing biotite in the Sarnowsar granitic rocks. Values of the log (fH_2O/fHF) range from 3.38 to 4.43 and values of the log ($fH_2O/fHCl$) range from 0.57 to 1.21 (Fig. 5). X_{Mg} (mole fraction of phlogopite in biotite) was plotted against the log (X_F/X_{OH}) and log (X_{Cl}/X_{OH}) (Fig 5). The log (fH_2O/fHF) and log ($fH_2O/fHCl$) values are shown in Fig. 5 by the parallel lines. The lines representing log (fH_2O/fHF) values are slightly different with the slope of trend of biotite composition suggesting the chemical structure of biotite playa a main role in the incorporation of F in biotite (Fig. 5-a). However, log (fH_2O/fHF) from contour line 4 toward contour line 3 reflect enrichment of F in fluid in equilibrium with the biotite, suggesting that the chemical composition of biotite also plays some role in the incorporation of F in biotite. In contrast with F, the lines representing log ($fH_2O/fHCl$) values are cut by biotite composition. The Cl content in the biotites has a very different trend with log ($fH_2O/fHCl$) parallel lines, which are predicted by thermodynamic data (Fig. 5-b). If the biotites are in equilibrium with the same fluid composition and at the same temperature, then their Cl content trend should be along the parallel lines which represent log($fH_2O/fHCl$) in Fig. 5-b. Therefore, distribution of data in Fig. 5 that cross the iso-fugacity ratio contours indicates that these should be due to variations in the composition of fluid or temperatures. Such variations are usually ascribed to variation in fluid composition rather than to a difference in temperature. The fugacities calculated at other temperatures in this study and also mentioned

by Munoz [1] and Middelaar and Keith [2], a temperature difference about 200° C or more would be required to get observed variations in the fugacities.

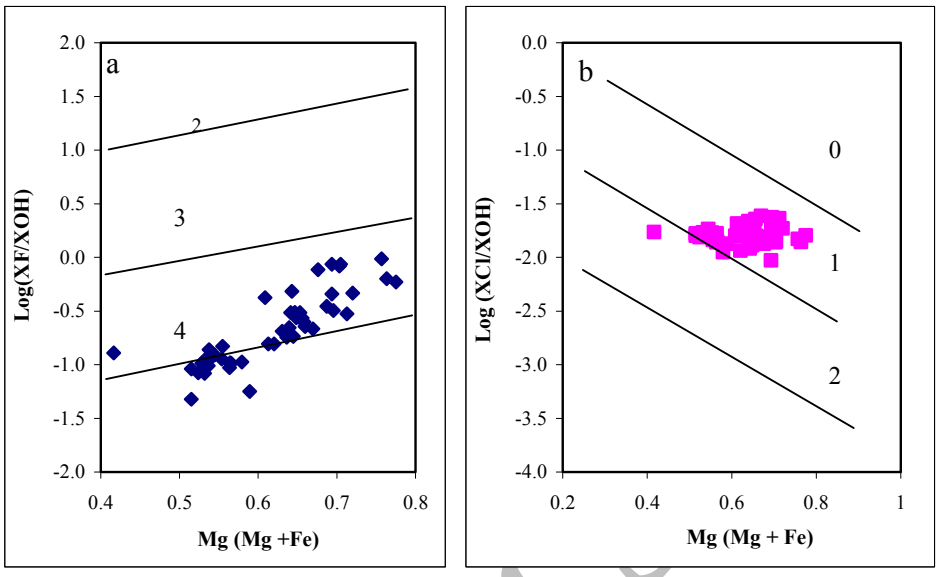

Fig. 5. (a) plot of Mg/(Mg + Fe) versus log (X_F/X_{OH}) for biotite from the Sarnowsar granite. Parallel lines (contours) show values of log (fH_2O/fHF) that were calculated assuming the equilibrium of fluid with the biotite at 727° C. (b) Plot of Mg/(Mg + Fe) versus log (X_F/X_{Cl}) for biotite from the Sarnowsar granite. Parallel lines (contours) show values of log ($fH_2O/fHCl$) that were calculated assuming the equilibrium of fluid with the biotite at 727° C

7. FLUORINE AND CHLORINE INTERCEPT VALUES

F and Cl intercept values were introduced to define a single numerical value, which expresses the relative degree F or Cl enrichment in a mica [1]. The F and Cl intercept value are temperature independent and are useful to compare the halogen contents in micas with different composition [1]. The F intercept value IV(F) and IV(Cl) for biotite are defined by the following equations:

$$IV(F)biotite=1.52X_{Mg}+0.42X_{An}+0.20X_{Sid}-\log (X_F/X_{OH})$$

$$IV(Cl)biotite=-5.01-1.93X_{Mg}-\log (X_{Cl}/X_{OH})$$

Rearrangement of the above equations leads to expressions that relate the water-halogen fugacity ratio in the fluid to the composition of the mica as follows [1]:

$$\log (fH_2O/fHF) = 2100/T+IV(F)$$

$$\log (fH_2O/fHCl) = 5151/T+IV(Cl)$$

These intercept values relate the fluorine and chlorine fugacity in the fluid to the composition of fluid [1]. The F intercept value IV(F) for biotite in the Sarnowsar granitic rocks are presented in Table 3 and Fig 6. The F intercept for biotite in the Sarnowsar granitic rocks is similar to those of igneous rocks and porphyry Cu ore deposits (Table 4). In contrast, the Cl intercept value of biotite in the Sarnowsar granitic rocks (Table 3, Fig. 7) is similar to those of hydrothermal systems and different to those of igneous rocks (Table 4). The data suggest that chlorine intercept values for biotite from the Sarnowsar granite tend to be more negative (more Cl rich) compared to Cl values in biotites from other igneous rocks. Smaller fluorine intercept values are correlated with higher relative degrees of fluorine enrichment in fluid and more negative chlorine intercept values correlate with higher chlorine enrichment.

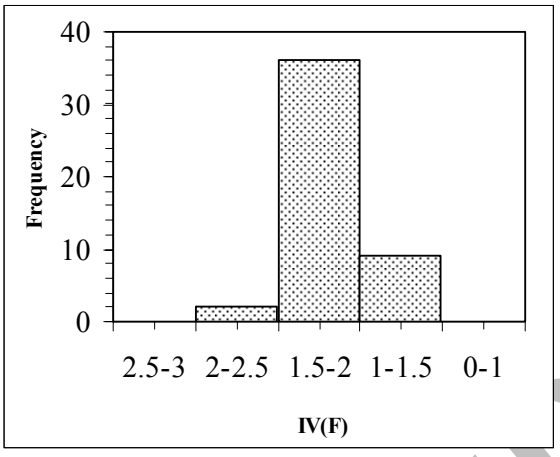

Fig. 6. Histogram of F intercept value (IV(F)) for biotites from the Sarnowsar granite

Table 4. Comparison IV(F), IV(Cl) and IV(F) of the Sarnowsar granite and other area

	IV(F)	-IV(Cl)	IV(F/Cl)	References
Sarnowsar granite	2.25-1	4.75-4	6.5-5.5	-
Igneous rocks	2.5-1.5	4.25-3	-	[1]
Santa r Rita (Porphyry Cu)	2.25-1.75	4.5-4	-	[1]
Other porphyry Cu	2.75-1.5	5-3.5	6.75-5.5	[1]
Sn-W-Be	2.-0.5	4.25-3.5	6-4.5	[1]
Henderson (Porphyry Mo)	1-0.25	4.5-3.75	5.75-4	[1]

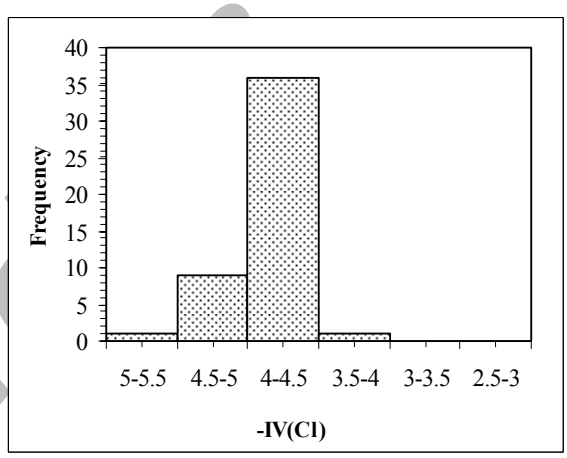

Fig. 7. Histogram of Cl intercept value (IV(Cl)) for biotites from the Sarnowsar granite

The fluorine-chlorine intercept value defined and calculated for biotite by combining the above two equations as shown below [1]:

$$\log (f\mathrm{HCl}/f\mathrm{HF})=-3051/T+\mathrm{IV(F)}-\mathrm{IV(Cl)}=-3051/T+\mathrm{IV(F/Cl)}$$

$$\mathrm{IV(F/Cl)}=3.45\ X_{Mg}+0.41X_{An}+0.20X_{Sid}-\log (X_F/X_{Cl})+5.01$$

The F/Cl intercept values of biotite in the Sarnowsar granitic rocks are present in Table 3 and Fig. 8 as a histogram and are plotted against IV(F) in Fig 9. The F/Cl intercept values are directly related to the fugacity ratio f(HCl)/f(HF) because it is independent of the temperature of equilibrium and the OH content of the mica [1]. Lower IV(F/Cl) values correspond to a higher F/Cl ratio. The F/Cl intercept value

from biotite in the Sarnowsar granitic rocks are similar to porphyry copper deposits that are more Cl rich than the other two types (from comparison with Table 4). Some biotites in the Sarnowsar granitic rocks have very high contents of F in composition (4.39 wt %). Such F-rich biotites in the Sangan biotite are not common, even in F-rich granitic systems. However, F-rich biotites and both F-poor biotites from the Sangan deposit show similar and narrow ranges of F/Cl intercept values corresponding to Cl-rich systems rather than F-rich systems (Table 4). These discussions indicate that incorporation of F in biotite in the Sarnowsar granitic rocks were mainly controlled by X_{Mg} in octahedral sites of biotites. In contrast, incorporation of Cl in biotite from the Sarnowsar granitic rocks was mainly controlled by chemical composition of fluid. Therefore the chemical composition of biotite from the Sarnowsar granite interacted with hydrothermal solutions.

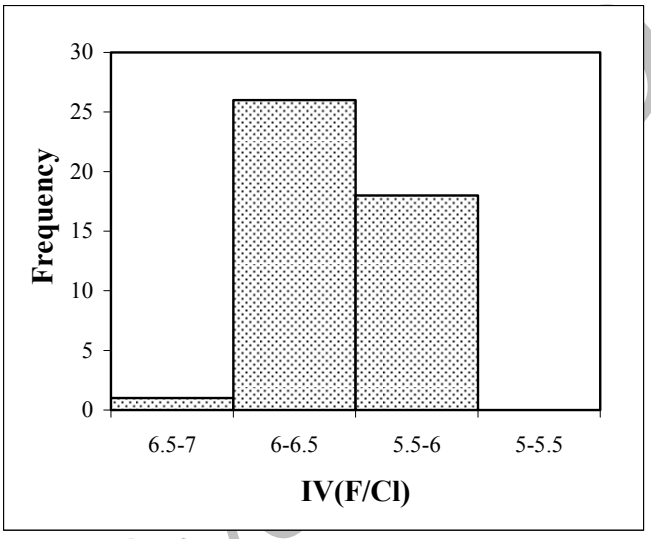

Fig. 8. Histogram of F/Cl intercept value (IV(F/Cl)) for biotites from the Sarnowsar granite

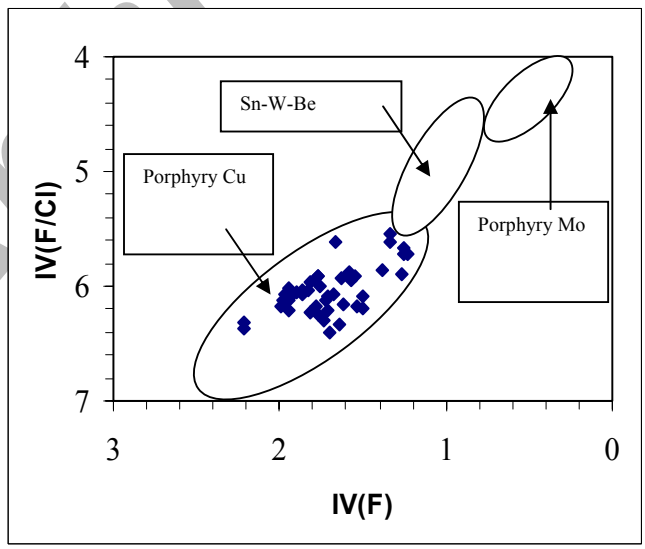

Fig. 9. F/Cl intercept value plotted against F intercept value for biotite from the Sarnowsar granite. The fields are modified from [1]. Composition of biotite from the Sarnowsar granite is similar as those of porphyry Copper deposits

8. RELATIONSHIPS BETWEEN HOST GRANITE CHEMISTRY AND HALOGEN CONTENTS IN BIOTITE

There are also some relationships between major elements in whole rock samples from the granite and halogen in the biotite. The correlations show a consistency with the crystallization trend. As shown in Fig. 10, with increasing Si in the magma, F contents in the biotite increase and Cl contents in the biotite decrease. The content of F in the biotite is positively correlated with K and content of Cl in the biotite is positively correlated with Na in the granite whole rock. These relationships may suggest evolution and separation of an aqueous phase from the Sangan granite. The volatile element of chlorine ion (Cl^-), is partitioned strongly toward the magmatic aqueous phase [34] because chloride minerals are not stable in magmas of intermediate to felsic compositions, and form highly stable, neutral chloride complexes with hydrogen, alkali metals, alkaline earths, and heavy metals in aqueous solutions at magmatic temperatures and low to moderate pressures [35]. Fluorine also forms stable neutral fluoride complexes in magmatic fluids, but high solubility fluorine in silicate melts cause fluorine to be partitioned largely in melts and hydrous minerals [35]. During differentiation of granite melt, CaO, FeO, MgO, MnO and TiO_2 are removed from the magma, the F, Cl, and H_2O concentration of magma increase until the magma becomes saturated with respect to a fluid phase [3]. Therefore, negative correlation between F and Cl in the Sarnowsar granitic rocks (Fig. 4) suggest that a Cl rich fluid evolved from the melt. As already shown, the F/Cl intercept values from biotite in the Sarnowsar granitic rocks indicate Cl rich systems. Quartz in the Sarnowsar granitic rocks, quartz vein in scapolitic hornfels adjacent to the Sarnowsar granite and interstitial calcite in garnets of the Sangan ore deposit contain high salinity fluid inclusions [26]. Hastingsite and scapolite in the Skarn zones of the Sangan iron deposit are also rich in Cl [36]. Such evidence shows that the granite had been in equilibrium with a Cl rich hydrothermal fluid. If the magma crystallized at pressures $\leq$ 2 kbar, then the magma could not have undergone extensive crystallization prior to water saturation. Under these conditions and with a concentration of F $\leq$ 1.8 and with a concentration of Cl only=0.26 is that if a magmatic hydrothermal fluid evolved, F partitioned in favor of the magma and Cl partitioned strongly in favor of the fluid [3].

The normative compositions of the Sarnowsar granitic rocks in the system Q-Ab-An-H_2O trend toward Ab, indicating lower temperature minimum point [26]. This is caused by high water pressure or by high F ratio [37, 13]. F-rich biotites in the Sangan granite rocks my be expected to form from an F-rich melt and the normative composition of the Sarnowsar granitic rocks that tend toward the Ab side may be expected due to a high F ratio rather than high water pressure. However, F in the biotite has a negative correlation with modal % of plagioclase and biotite (Fig. 10). Therefore, variation of F contents in the biotite is strongly dependent on the modal percent of the biotite, because more than 70 to 90 % of F in melt can be substituted for a biotite structure [5]. Therefore, the trend of the normative composition of the Sarnowsar granitic rocks toward the Ab side can be also due to high H_2O pressure. The biotite and amphibole textures, granodioritic and dioritic facies in marginal parts, normative compositions, fluid inclusions with several daughter minerals and halogen contents of the Sangan granites show that the melt contained enough water and was volatile. A minimum of 2.7 wt % of H_2O in the initial melt required operating a magmatic phase during crystallization and emplacement in shallow parts of the crust [35].

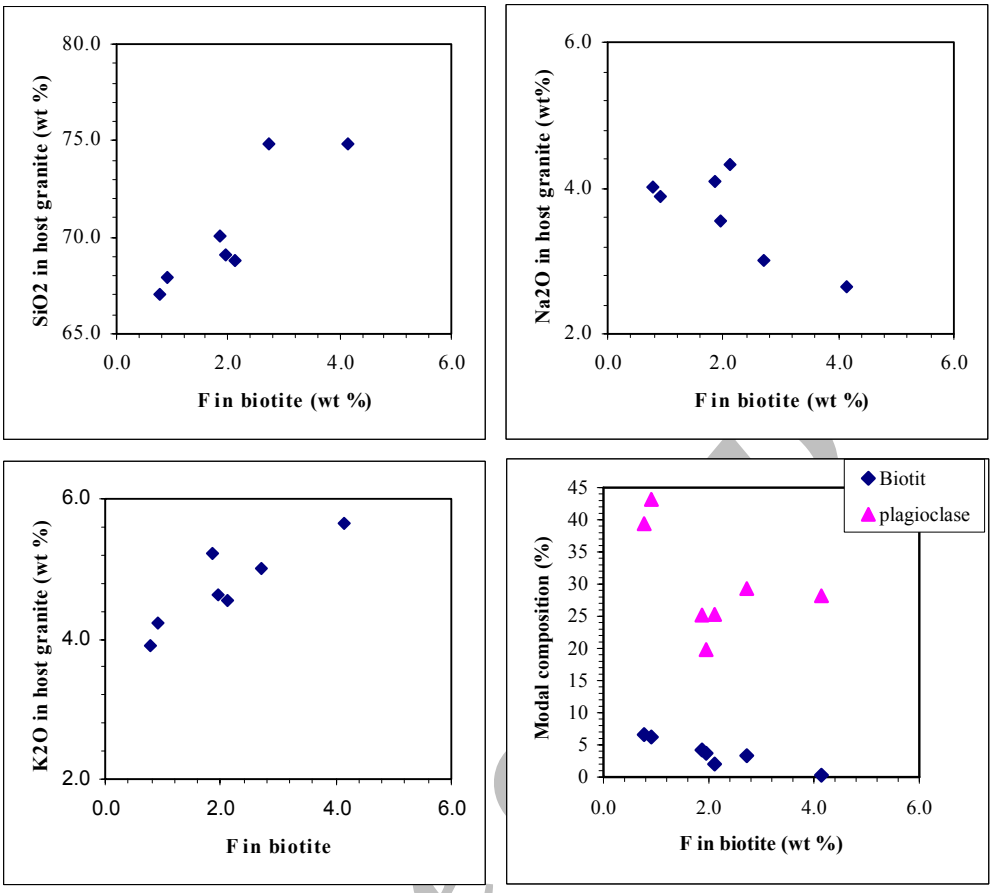

Fig. 10. Relationship among wt % of F in biotite with wt % SiO_2 (a), Na_2O (b) and K_2O (c) of whole rock samples of the host granite and modal % of biotite and modal % of plagioclase (d)

9. CONCLUSIONS: HALOGENS IN GRANITE

1. X_{Mg} in biotite from the Sarnowsar granitic rocks is positively correlated with F and has weak negative correlation with Cl contents.
2. The log (fH_2O/fHF) values of fluid in equilibrium with the biotite composition indicate that the chemical structure of biotite plays the main role in incorporation of F in the biotite, however, the chemical composition of the fluid also plays some role.
3. The log ($fH_2O/fHCl$) values of fluid in equilibrium with the biotite composition indicate that the chemical composition of the fluids plays the main role in variation of Cl in the biotite.
4. The F intercept for biotite in the Sarnowsar granitic rocks is similar to those of igneous rocks and porphyry Copper ore deposits. The Cl intercept value of biotite in the Sarnowsar granitic rocks is similar to those of hydrthermal systems. The data suggest that chlorine intercept values for biotite from the Sarnowsar granite tend to be more Cl rich than comparable values from biotites in common igneous rocks. F-rich biotites and F-poor biotites from the Sarnowsar granite show similar and narrow ranges of F/Cl intercept values corresponding to Cl-rich systems rather than F-rich systems.
5. The trend is for the fluorine contents of biotites to increase and the chlorine contents to decrease with an increase in the silica content of the host granitic rocks. This may suggest that Cl partitions preferentially into aqueous fluid. Therefore, there should be a fluorine rich melt associated with a Cl-Na-rich magmatic aqueous fluid phase.

REFERENCES

1. Munoz, J. L. (1984). F-OH and Cl-OH exchange in mica with application to hydrothermal ore deposits. *Rev. Mineral., 13*, 469-493.
2. Middelaar, W. T. & Keith, J. D. (1990). Mica chemistry as an indicator of oxygen and halogen fugacities in the CanTung and other W-related granitoids in the North American Cordillera. *Geol. Soc. of Ameri. Speci*. 246.
3. Webster, J. D. (1990). Partitioning of Cl between magamatic hydrothermal fluids and highly evolved granitic mamas. *Geol. Soc. of Ameri. Speci*. 246.
4. Candela, P. A. (1997). A review of shallow, ore related granites: Textures, volatiles and ore metal. *Journal of petrology, 38*(12), 1619-1633.
5. Speer, A. (1984). Micas in igneous rocks. *Rev. Mineral., 13*, 299-356.
6. Munoz, J. L. & Ludington, S. D. (1977). Fluoride-hydroxyl exchange in synthetic muscovite and its application to muscovite-biotite assemblages. *Amer. Mineral., 62*, 304-308.
7. Munoz, J. L. & Swenson, A. (1981). Chloride-hydroxyl exchange in biotite and estimation of relative HCl/HF activities in hydrothermal fluids. *Econ. Geol., 76*, 2212-2221.
8. Ramberg, H. (1952). Chemical bonds and distribution of cations in silicates. *J. Geol. 60*, 331-335.
9. Ekstrom, T. K. (1972). The distribution of fluorine among some coexisting minerals. *Contrib. Mineral Petrol., 34*, 192-200.
10. Stormer, J. C. & Carmichael, I. S. E. (1971). Fluorine-hydroxyl exchange in apatite and biotite: A potential igneous geothermometer. *Contr. Mineral. Petrol., 31*, 121-131.
11. Zaw, U. K. & Clark, A. H. (1978). Fluoride-Hydroxyl ratios of skarns silicates, Cantung E-zone scheelite orebody, Tungsten, Northwest Territories. *Canadian Mineral, 16*, 207-221.
12. Nedachi, M. (1980). Chlorine and fluorine contents of rock-forming minerals of the Neogene granitic rocks in Kyushu, Japan. *Mining Geol. Spec. Iss., 8*, 39-48.
13. Manning, D. A. C. (1981). The effect of fluorine on liqudus phase relationships in the system Qtz-Ab-Or with Excess Water at 1 kb. *Contrib. Mineral, Petrol., 76*, 206-215.
14. Munoz, J. L. (1990). F and Cl contents of hydrothermal biotites: A reevaluation. *GSA Abst. Prog. 22*, A135.
15. Zhu, C. & Sverjensky, D. A. (1991). Partitioning of F-Cl-OH between minerals and hydrothermal fluids. *Geochim. Cosmochim. Acta, 55*, 1837-1858.
16. Zhu, C. & Sverjensky, D. A. (1992). Partitioning of F-Cl-OH between biotite and apatite. *Geochim. Cosmochim. Acta, 56*, 3435-3467.
17. Icenhower, J. P. & London, D. (1997). Partitioning of fluorine and chlorine between biotite and granitic melt: experimental calibration at 200 Mpa H2O. *Contrib. Mineral, Petrol., 127*, 17-29.
18. Sallet, R. (2000). Fluorine as a tool in the petrogeneesis of quartz-bearing magmatic associations: applications of an improved F-OH biotite-apatite thermometer grid. *Lithos, 50*, 241-253.
19. Seifert, W., Kampf, H. & Wasternack, J. (2000). Compositional variation in apatite, phlogopite and other accessory minerals of the ultramafic Delitzsch complex, Germany: implication for cooling history of carbonatites. *Lithos, 53*, 81-100.
20. Li, Z., Tainosho, Y., Shiraishi, K. & Owada, M. (2003). Chemical characteristics of fluorine-bearing biotite of early Paleozoic plutonic rocks from the Sor Rondane Mountains, East Antarctica. *Geochemical Journal, 37*, 145-161.
21. Sisson, V. B. (1987). Halogen chemistry as an indicator of metamorphic fluid interaction with the Ponder pluton, Coast plutonic Complex, British Columbia, Canada. *Contrib. Mineral, Petrol., 95*, 123-131.
22. Stocklin, J. (1968). Structural history and tectonics of Iran, a review. *Amirican Association of Petroleum Geologists Bulletin, 52*(7), 1229-1258.
23. Berberian, M. & King, G. C. (1981). Towards a paleogeography and tectonic evolution of Iran. *Can. J. Earth*

Sci., 18, 210-265.

24. Alavi, M. (1994). Tectonic of the Zagros orogenic belt of Iran: new data and interpretations. *Tectonophysics, 229*, 211-238.
25. Walker, R. & Jackson, J. (2002). Offset and evolution of the Gowk fault, S.E, Iran: a major intra-continental strike-slip system, *Journal of Structural Geology, 24*, 1677-1698.
26. Boomeri, M. (1998). Petrography and geochemistry of the Sangan iron skarn deposit and related igneous rocks, northeastern Iran. Unpublished Ph.D. thesis, Akita University, Japan, 226pp.
27. Hezarkhani, A. & Williams-Jones, A., E. (1998). Controls of alteration and mineralization in the Sungun porphyry copper deposit, Iran: Evidence from fluid inclusions and sTable isotopes. *Econ. Geol., 93*, 651-670.
28. Ternet, Y. (1990). Explanatory text of the Taybad quadrangle map 1/250000. Ministry of mines and metals, *geological survey of Iran, Tehran*, 200.
29. Alavi Naini, M. (1980). Geological quadrangle map of Khaf: series sheet 8059, Ministry of mines and metals. *Geological survey of Iran, Tehran*.
30. Wones, D. R. (1989). Significance of the assemblage titanite + magnetite + quartz in granitic rocks, *Amer. Mineral., 74*, 744-749.
31. Munoz, J. L. & Ludington, S. D. (1974). Fluoride-hydroxyl exchange in biotite. *Am. J. Sci., 274*, 396-413.
32. Gunow, A. J., Ludington, S. & Munoz, J. L. (1980). Fluorine in micas from the Henderson molybdenite deposits, Colorado. *Econ. Geol., 75*, 1127-1137.
33. Whitney, J. A. (1989). Origin and evolution of silicic magmas. *Reviews in Economic geology, 4*, 183-201.
34. Kilinc, I. A. & Burnham, C. W. (1972). Partitioning of chloride between a silicate melt and coexisting aqueous phase from 2 to 8 kilobars. *Econ. Geol., 67*, 231-235.
35. Burnham, C. W. & Ohmoto, H., (1980). Late-stage processes of felsic magmatism. *Mining Geol. Spec. Iss., 8*, 1-11.
36. Boomeri, M., Mizuta, T., Nakashima, K., Ishiyama, D. & Ishikawa, Y. (1997). Geochemical characteristics of halogen-bearing hastingsite, scapolite and phlogopite from the Sangan iron skarn deposits, northeastern Iran. *J. Min. Pet. Econ. Geol of Japan, 92,* 481-501.
37. Tuttle, O. F. & Bowen, N. I. (1958). Origin of granite in the light of experimental studies in the system $NaAl_3O_8$-$KAlSi_3O_8$-SiO_2-H_2O. *Geol. Soc. of Ameri. Memori 74*, 153.